BJ Cell

Biochem. J. (2015) **469**, 83–95 doi:10.1042/BJ20150072

Critical role of evolutionarily conserved glycosylation at Asn^{211} in the intracellular trafficking and activity of sialyltransferase ST3Gal-II

Fernando M. Ruggiero*, Aldo A. Vilcaes*, Ramiro Iglesias-Bartolomé† and José L. Daniotti*[1]

*Centro de Investigaciones en Química Biológica de Córdoba (CIQUIBIC, UNC-CONICET), Departamento de Química Biológica, Facultad de Ciencias Químicas, Universidad Nacional de Córdoba, Córdoba, Argentina

†Oral and Pharyngeal Cancer Branch, National Institute of Dental and Craniofacial Research, National Institutes of Health, Bethesda, MD 20892, U.S.A.

ST3Gal-II, a type II transmembrane protein, is the main mammalian sialyltransferase responsible for GD1a and GT1b ganglioside biosynthesis in brain. It contains two putative N-glycosylation sites (Asn^{92} and Asn^{211}). Whereas Asn^{92} is only conserved in mammalian species, Asn^{211} is highly conserved in mammals, birds and fish. The present study explores the occupancy and relevance for intracellular trafficking and enzyme activity of these potential N-glycosylations in human ST3Gal-II. We found that ST3Gal-II distributes along the Golgi complex, mainly in proximal compartments. By pharmacological, biochemical and site-directed mutagenesis, we observed that ST3Gal-II is mostly N-glycosylated at Asn^{211} and that this co-translational modification is critical for its exit from the endoplasmic reticulum and proper Golgi localization. The individual N-glycosylation sites had different effects on ST3Gal-II enzymatic activity. Whereas the *N*-glycan at position Asn^{211} seems to negatively influence the activity of the enzyme using both glycolipid and glycoprotein as acceptor substrates, the single *N*-glycan mutant at Asn^{92} had only a moderate effect. Lastly, we demonstrated that the N-terminal ST3Gal-II domain containing the cytosolic, transmembrane and stem region (amino acids 1–51) is able to drive a protein reporter out of the endoplasmic reticulum and to retain it in the Golgi complex. This suggests that the C-terminal domain of ST3Gal-II depends on N-glycosylation to attain an optimum conformation for proper exit from the endoplasmic reticulum, but it does not represent an absolute requirement for Golgi complex retention of the enzyme.

Key words: ganglioside, glycolipid, Golgi complex, *N*-glycan trimming, N-glycosylation, sialyltransferase, ST3Gal-II.

INTRODUCTION

Gangliosides consist of a lipid anchor, the ceramide, decorated by a glycan chain of variable length and structure. In cells, gangliosides are embedded in the outer leaflets of the plasma membrane through their ceramide moiety, exposing the oligosaccharide portion to the extracytoplasmic side. These glycolipids have been implicated in many physiological processes, including growth, differentiation, migration and apoptosis, through modulating both cell signalling processes and cell–cell and cell–matrix interactions. Moreover, gangliosides have been associated with a wide range of pathological processes, being receptors for viruses, toxins, lectins and antibodies [1–3].

The synthesis of gangliosides starts in the endoplasmic reticulum compartment with the synthesis of the ceramide, the common precursor of all gangliosides. Aided by the ceramide-transfer protein, CERT, ceramide is then transferred to the Golgi complex, and thereafter converted into glucosylceramide. Subsequently, other carbohydrate residues are attached, one by one, catalysed by glycosyltransferases, as described in Figure 1.

The level of expression and diversity of gangliosides can be controlled by regulating the sugar nucleotide and acceptor availability and by enzymatic degradation, as well as through the presence and activity of the glycosyltransferases that participate in their biosynthesis. Different types of regulation of glycosyltransferases have been reported, i.e. transcriptional, translational or post-translational [1,2,4]. More recently, an additional type of regulation of glycolipid expression has been shown to occur at the plasma membrane level, due to plasma-membrane-associated ectoglycohydrolases and glycosyltransferases [5–7].

N-linked protein glycosylation is one of the most frequent co- and post-translational protein modifications in eukaryotes, with more than half of all eukaryotic proteins predicted to be N-glycoproteins [8]. N-glycosylation is initiated by a co-translational process in the lumen of endoplasmic reticulum. The *N*-glycans are added to the side-chain amide of asparagine residues in the conserved sequon Asn-Xaa-(Thr/Ser) (where Xaa≠Pro), and further trimmed and remodelled upon transit through the Golgi. N-glycosylation of proteins has multiple effects, ranging from intracellular sorting to regulation of half-life and bioactivity [9,10]. However, many proteins that are normally glycosylated show no loss of function when glycosylation is prevented [11–13].

Sialyltransferases are a group of glycosyltransferases that use CMP-Neu5Ac (cytidine 5′-monophospho-*N*-acetylneuraminic acid) as a donor substrate to catalyse the transfer of sialic acid to oligosaccharide chains from glycolipids and glycoproteins. They are classified as ST3Gal, ST6Gal, ST6GalNAc and ST8Sia families on the basis of the linkage in which sialic acid is transferred and the acceptor saccharide [14]. Sialyltransferases are type II integral membrane proteins with an N-terminal domain consisting of a relatively short cytoplasmic tail facing the cytoplasm, a transmembrane uncleaved signal-anchor region and

Abbreviations: BFA, brefeldin A; CHO-K1, Chinese-hamster ovary K1; CMP-Neu5Ac, cytidine 5′-monophospho-*N*-acetylneuraminic acid; DMEM, Dulbecco's modified Eagle's medium; Endo H, endoglycosidase H; GM130, *cis*-Golgi matrix protein of 130 kDa; HA, haemagglutinin; HPTLC, high-performance TLC; M6PR, mannose 6-phosphate receptor; PNGase F, peptide N-glycosidase F; ST3Gal, α2,3-sialyltransferase; TGN, *trans*-Golgi network; TTBS, TBS containing 0.5 % Tween 20.

[1] To whom correspondence should be addressed (email daniotti@dqb.fcq.unc.edu.ar).

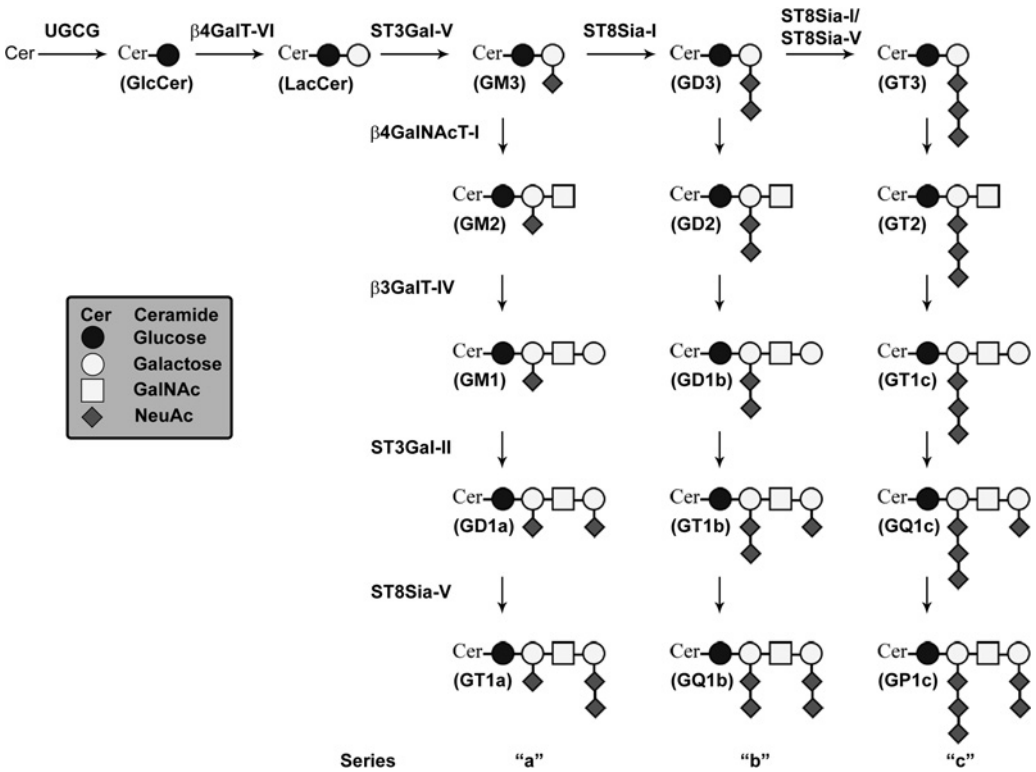

Figure 1 Scheme of the biosynthesis of oligosaccharide moieties of gangliosides

Transfer steps for synthesis of a-, b-, and c-series gangliosides are shown. UGCG, UDP-Glc:ceramide glucosyltransferase; β4GalT-VI, UDP-Gal:glucosylceramide galactosyltransferase; ST3Gal-V, CMP-NeuAc:lactosylceramide sialyltransferase (also called Sial-T1); ST8Sia-I, CMP-NeuAc:GM3 sialyltransferase (also called Sial-T2) and CMP-NeuAc:GD3 sialyltransferase; β4GalNAcT-I, UDP-GalNAc:lactosylceramide/GM3/GD3/GT3 N-acetylgalactosaminyltransferase (also called GalNAc-T); β3GalT-IV, UDP-Gal: GA2/GM2/GD2/GT2 galactosyltransferase (also called Gal-T2); ST3Gal-II, CMP-NeuAc:GA1/GM1/GD1b/GT1c sialyltransferase (also called Sial-T4); ST8Sia-V, CMP-NeuAc:GM1b/GD1a/GT1b/GQ1c sialyltransferase and CMP-NeuAc:GD3 sialyltransferase. Gangliosides are named according to Svennerholm [53].

a luminally oriented C-terminal domain that bears the catalytic and the sugar nucleotide-binding sites. Sialyltransferases are mainly localized at the Golgi complex. However, the presence of these glycosyltransferases at the cell surface has also been demonstrated [5,7,15,16].

The mouse and human genomes encode six ST3Gal (α2,3-sialyltransferase) enzymes (ST3Gal-I to ST3Gal-VI). They catalyse the formation of a α2,3-linkage between Neu5Ac and terminal galactose residues found both on glycoproteins and glycolipids. In particular, ST3Gal-I and ST3Gal-II catalyse *in vitro* the addition of sialic acid to the terminal galactose of Galβ1-3GalNAc-terminated glycolipids, which are comparatively the preferred substrates for ST3Gal-II [17,18]. The amino acid sequence of human ST3Gal-II shows 49 % similarity to human ST3Gal-I and 93.7 % similarity to murine ST3Gal-II. Comparison of the substrate specificities of human and murine ST3Gal-II showed that both enzymes exhibit close substrate specificity except for asialoglycoproteins containing the Gal(β1-3)GalNAc terminal sequence that were better substrates for the human enzyme [19]. In contrast with mammalian ST3Gal-II, a related sialyltransferase from the Japanese pufferfish *Takifugu rubripes* (Q6KB57; now called ST3Gal-VIII [20]), exhibits activity towards the disaccharide Galβ1-3GalNAc and asialofetuin, but not GM1 or GD1b gangliosides [21]. In this regard, the ceramide-binding/recognition site proposed for mouse ST3Gal-II [22] may represent a unique feature of mammalian ST3Gal-II that is lacking in evolutionarily more distant species such as fish [21].

Recently, it was clearly demonstrated by genetic experiments in mouse that ST3Gal-II is the main mammalian sialyltransferase responsible for GD1a and GT1b ganglioside biosynthesis in the brain *in vivo* [23]. In addition, ST3Gal-II activity on glycoprotein substrates was also reported [19,23]. Interestingly, ST3Gal-II, one of the few glycosyltransferases reported to date that are capable of transferring to different monosaccharide residues [24], is the first sialyltransferase described to catalyse 'reversible sialylation', which involves the enzymatic transfer of NeuAc from linear and sialylated donors to the acceptor CMP resulting in the formation of CMP-NeuAc [25].

As for other mammalian glycosyltransferases, the primary amino acid sequence of ST3Gal-II reveals one potential N-glycosylation site (Asn^{211}) which is highly conserved in human, mouse, rat, cattle, monkey, chicken and fish. However, another potential N-glycosylation site (Asn^{92}) observed in ST3Gal-II sequence is only conserved in mammalian species (Figures 2B and 2C). Whether these glycosylation sequons are occupied by oligosaccharides is unknown, so information on the possible influences of carbohydrates on ST3Gal-II activity, stability and intracellular traffic, as well as subcellular distribution, is lacking.

In the present study, we first examined the precise sub-Golgi localization and the occupancy of N-glycosylation sites of human ST3Gal-II. Additionally, we studied the effect of inhibiting *en bloc* glycosylation and oligosaccharide trimming on the activity and intracellular distribution of the enzyme.

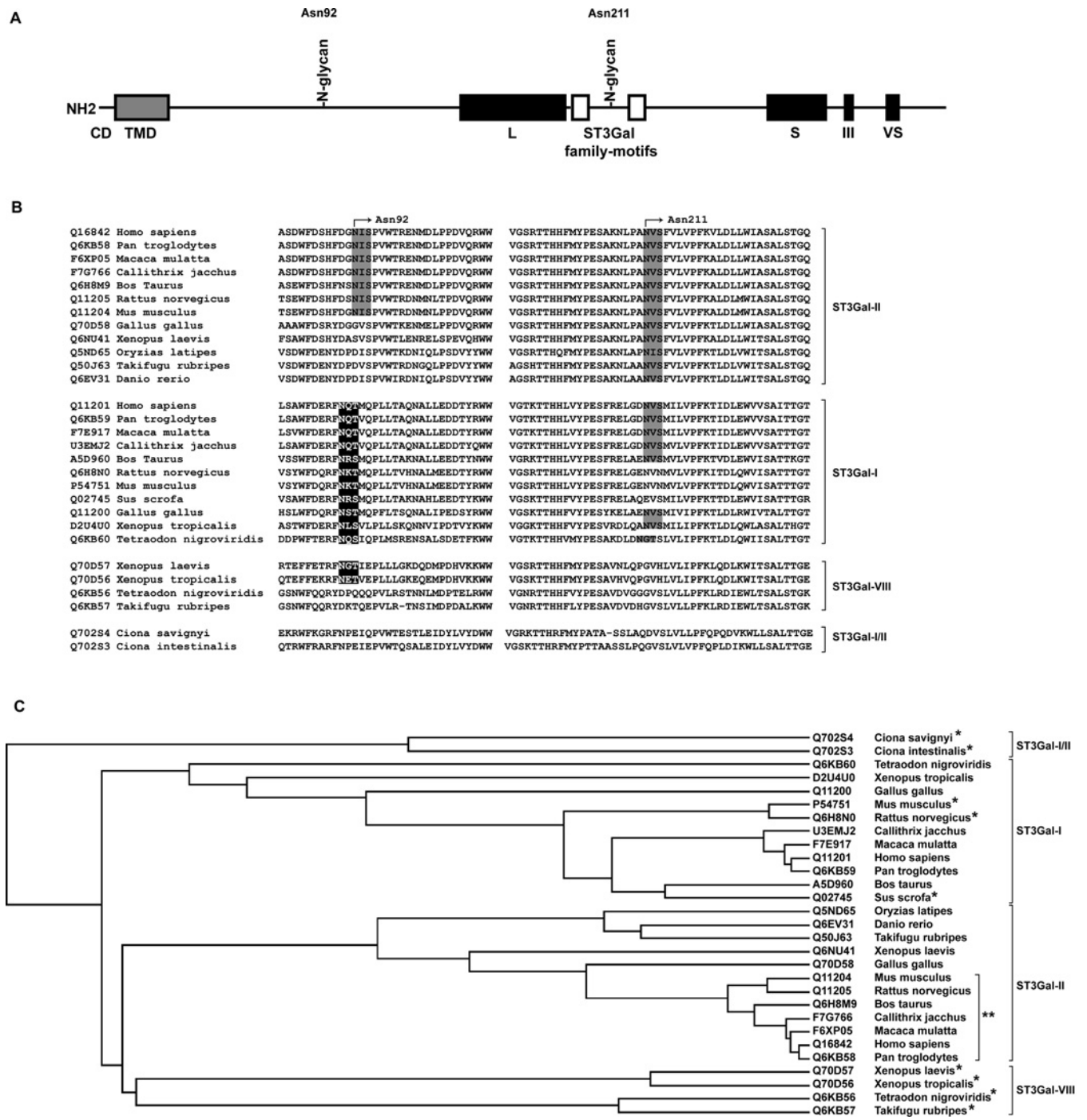

Figure 2 N-glycosylation site analysis of sialyltransferases from ST3Gal family

(**A**) Schematic representation of primary amino acid sequence of human ST3Gal-II showing putative *N*-glycan positioning at the two potential N-glycosylation sites Asn^{92} and Asn^{211}. The sialyltransferase superfamily conserved sialylmotifs L (large), S (small), III and VS (very small) are represented by black boxes. The conserved ST3Gal family motifs are represented by white boxes. CD, cytoplasmic domain; TMD, transmembrane domain. (**B**) Alignment of reported ST3Gal-I, II, I/II and VIII sequences. Alignment of the primary amino acid sequence by Clustal Omega software (http://www.uniprot.org/align) reveals that the potential N-glycosylation site at Asn^{211} (NVS sequon) is absent from ST3Gal-I/II and ST3Gal-VIII, but highly conserved in ST3Gal-I and ST3Gal-II sequences (grey box) with the exception of pig, mouse and rat ST3Gal-I. In contrast, the potential N-glycosylation site at Asn^{92} (NIS sequon) is conserved only in ST3Gal-II from mammalian species (grey box). Less conserved potential N-glycosylation sequons are also found near this position in vertebrate ST3Gal-I (NQT/NRS/NKT/NST/NLS/NQS) and ST3Gal-VIII *Xenopus* sequences (NGT/NET) (black box). (**C**) Phylogenetic tree of the reported ST3Gal-I, II, I/II and VIII sequences. *Absence of the potential N-glycosylation site at Asn^{211} (NVS sequon). **Conservation of the potential N-glycosylation site at Asn^{92} (NIS sequon).

EXPERIMENTAL

Plasmids and site-directed mutagenesis

The plasmid coding for the human ST3Gal-II tagged at the C-terminus with the epitope c-myc (pCi-hST3Gal-II-myc) was synthesized by Genscript. To generate pCEFL2-hST3Gal-II-HA, the human ST3Gal-II was subcloned into pCEFL2-HA, a modified pCEFL encoding the HA (haemagglutinin) nanopeptide epitope YPYDVPDYA. Single amino acid substitutions of glutamine for asparagine in ST3Gal-II (N92Q, N211Q and N92Q/N211Q) were made using pCEFL2-hST3Gal-II-HA as template and the QuikChange® site-directed mutagenesis kit (Stratagene). To generate pCEFL2-ST3Gal-II–cherry, which drives the expression of the first 51 amino acids from hST3Gal-II fused to cherry fluorescent protein, the corresponding cDNA fragment of ST3Gal-II was subcloned into pCherry plasmid (Clontech). The identity of each construct was confirmed by DNA sequencing. The MHC class II invariant chain isoform (Iip33) fused to YFP was gratefully received from H.J.F. Maccioni (CIQUIBIC, National University of Córdoba, Córdoba, Argentina).

Antibodies

The following antibodies were used for indirect immunofluorescence experiments: monoclonal mouse anti-GM130 (*cis*-Golgi matrix protein of 130 kDa) and mouse anti-TGN38 (*trans*-Golgi network 38) were from BD Biosciences, polyclonal rabbit anti-c-myc and monoclonal mouse anti-HA were from Sigma–Aldrich. Alexa Fluor® 488-conjugated goat anti-mouse IgG or Alexa Fluor® 546-conjugated goat anti-mouse IgG were from Santa Cruz Biotechnology.

Cell culture and transfection

CHO-K1 (Chinese-hamster ovary K1) cells (A.T.C.C., Manassas, VA, U.S.A.) were maintained at 37 °C, 5 % CO_2 in DMEM (Dulbecco's modified Eagle's medium) supplemented with 10 % (v/v) FBS and antibiotics (100 μg/ml penicillin and 100 μg/ml streptomycin). Cells were transfected with 0.5–1.0 μg/35-mm-diameter dish of the indicated plasmid using linear polyethyleneimine (2 μg/35-mm-diameter dish) (Sigma–Aldrich).

In addition, some experiments were also performed using a CHO-K1 clone stably transfected with a plasmid coding for the N-terminus of ST8Sia-I (amino acids 1–57 containing the cytosolic and transmembrane regions) fused to YFP [5,26].

To generate stable CHO-K1 cells expressing ST3Gal-II, pCi-hST3Gal-II-myc was transfected into CHO-K1 cells using polyethyleneimine as indicated above. Following 48 h of expression, the cells were cultured in DMEM containing 10 % (v/v) FBS and 1 mg/ml geneticin (G418). Colonies of stable transfectants were isolated and screened for ST3Gal-II protein expression by Western blotting and immunofluorescence.

Confocal immunofluorescence microscopy

Cells grown on coverslips were washed twice with DMEM, fixed in 1 % (w/v) paraformaldehyde in PBS for 10 min at room temperature, permeabilized with 0.1 % Triton X-100/200 mM glycine in PBS for 2 min at room temperature and blocked with 3 % (w/v) BSA in PBS for 60 min at room temperature. Then, cells were exposed for 12 h at 4 °C to a 1:3000 dilution of antibody against c-myc or with a 1:2500 dilution of antibody against HA. Secondary antibodies were Alexa Fluor® 488-conjugated goat anti-mouse IgG or Alexa Fluor® 546-conjugated goat anti-mouse IgG, both diluted to 1:1000. After final washes with PBS, cells were mounted in FluorSave reagent (Calbiochem/EMD Biosciences). Confocal images were collected using an Olympus Fluoview FV-1000 laser-scanning confocal microscope equipped with an argon/helium/neon laser and a ×63 1.4 numerical aperture oil-immersion objective. Single confocal sections of 0.8 μm were taken parallel to the coverslip (*xy* sections). Images were acquired and processed with the FV10 lsm image software and ImageJ software (NIH). Final images were compiled with Adobe Photoshop CS6. The fluorescence micrographs shown are representative of at least three independent experiments.

Inhibition of *en bloc* glycosylation and oligosaccharide trimming

CHO-K1 cells were transiently transfected with either 0.7 μg of pCi (mock-transfected) or pCi-hST3Gal-II-myc constructs. Then, tunicamycin (10 μg/ml) (Enzo) or castanospermine (75 μg/ml) (Enzo) were added to culture medium. At 15 h after transfection, cells were processed as indicated under Confocal immunofluorescence microscopy.

Endo H (endoglycosidase H) and PNGase F (peptide N-glycosidase F) digestions

For digestion with Endo H, 30 μg of homogenate from ST3Gal-II expressing CHO-K1 cells was boiled for 10 min and then incubated in the presence or absence of 1.5 m-units of Endo H in 25 μl of a solution containing 0.1 M citrate buffer (pH 5.5), 0.5 % SDS and 0.1 M 2-mercaptoethanol for 18 h at 37 °C. For digestion with PNGase F, 30 μg of homogenate from cells transiently expressing wild-type or N-glycosylation mutant variants of ST3Gal-II were used for reaction according to the manufacturer's instructions (New England Biolabs) in the presence or absence of 1500 units of PNGase for 4 h at 37 °C in a final volume of 60 μl. In both digestions, reactions were stopped with SDS sample buffer and the products were analysed by Western blotting as indicated below.

ST3Gal-II enzyme activity assay

CHO-K1 cells transiently expressing the wild-type hST3Gal-II-HA or the enzyme carrying single- or double-asparagine mutation (N92Q, N211Q or N92Q/N211Q) were scrapped and resuspended in 50 μl of a solution containing 250 mM sucrose in 10 mM Tris/HCl (pH 7.2). The incubation system for enzymatic activity using glycolipid as acceptor substrate was performed in a final volume of 30 μl and contained 150 μg of protein from the cell extract, 400 μM GM1 (acceptor substrate), 17.6 μM CMP-9-fluoresceinyl-NeuAc (donor substrate, Glyco Medical Research), 20 mM $MnCl_2$, 1 mM $MgCl_2$, 75 μg of Triton CF54/Tween 80 (2:1 w/w) and 100 μM sodium cacodylate/HCl buffer (pH 6.5). Incubations were performed at 37 °C for 150 min. Reactions were stopped with 500 μl of chloroform/methanol (2:1, v/v) and samples were kept at room temperature for 20 min for lipid extraction. The lipid extracts were supplemented with appropriate amounts of standard gangliosides and chromatographed on HPTLC (high-performance TLC) plates (Merck) using chloroform/methanol and 0.25 % $CaCl_2$ (60:36:8, by vol.) as solvent. Standard gangliosides were visualized by exposing the plate to iodine vapour. Images were taken using an EC3 Bioimaging System (UVP) and analysed using ImageJ software.

A fluorimetric enzymatic assay was performed using glycoprotein as acceptor substrate [19,27]. The incubation system contained, in 30 μl of total volume, 50 μg of protein from the cell extract, 20 mM $MnCl_2$, 1 mM $MgCl_2$, 100 μM sodium cacodylate/HCl buffer (pH 6.5), 100 μM galactose and 25 μg Triton CF54/Tween 80 (2:1, w/w). Additionally, 6.3 μM CMP-9-fluoresceinyl-NeuAc plus 53.7 μM CMP-NeuAc (donor substrate) and/or 60 μg of asialofetuin (Sigma–Aldrich) were added to the incubation system. Reactions were performed at 37 °C for 120 min and stopped with 37.5 μl of chloroform/methanol (1:4, v/v). The precipitated proteins were washed twice with 30 μl of methanol and then resuspended in 300 μl of PBS solution containing 10 % sample buffer (4 % SDS, 50 mM Tris/HCl and 5 mM EDTA). Total fluorescence was measured using a FluoroMax-P Horiba Jobin Yvon spectrofluorimeter.

Western blotting

Total proteins were precipitated with chloroform/methanol (1:4, v/v) and quantified using the Bradford method. Then, 40 μg of total proteins per lane were resolved by SDS/PAGE and transferred on to nitrocellulose membrane. After incubation with 5 % (w/v) non-fat dried milk powder in TBS (50 mM Tris/HCl, pH 7.4, and 200 mM NaCl) for 60 min, the membrane was washed once with TBS and incubated with mouse monoclonal antibody against HA (1:1000) (clone HA-7, Sigma–Aldrich) at 4 °C for 12 h. Membranes were washed three times for 10 min with TTBS (TBS containing 0.5 % Tween 20) and incubated with a 1:10000 dilution of goat polyclonal antibody to mouse IgG (IRDye 800CW, LI-COR) for 1 h at room temperature. Blots were washed three times with TTBS and visualized using the LI-COR infrared imager system according to the manufacturer's protocols.

RESULTS

ST3Gal-II expression and sub-Golgi localization

To investigate the protein product of human ST3Gal-II cDNA and to learn its precise subcellular localization, we generated a plasmid able to direct the expression of the sialyltransferase tagged with the epitope HA at its C-terminus (pCEFL2-hST3Gal-II-HA). Extracts from ST3Gal-II-transfected CHO-K1 cells analysed by Western blotting showed ST3Gal-II with a molecular mass of 43 kDa (81 %) and 41 kDa (14 %), which probably correspond to the predicted molecular mass with or without one *N*-glycan respectively (Figure 3). A minor band of 45 kDa (2 %) had a molecular mass consistent with two *N*-glycans attached to the primary sequence (see below). No immunostained band was observed in extracts from mock-transfected CHO-K1 cells. It is worth mentioning that CHO-K1 cells synthesize mainly the simple ganglioside GM3 due to the lack of β4GalNAcT-I and ST8Sia-I activities. However, glycosyltransferases acting on GM2 to produce GM1 (β3GalT-IV) and GD1a (ST3Gal-I/ST3Gal-II) are constitutively present in these cells [28,29]. In gels run in the absence of 2-mercaptoethanol, a major band migrating at approximately 81 kDa was observed, which accounts for 50 % of the total enzyme (Figure 3). On the other hand, under reducing conditions, the 81 kDa form mostly disappeared and the concomitant appearance of the 43 and 41 kDa forms were observed. This result strongly suggested that the 81 kDa form is probably formed by a dimeric association via disulfide bridges of the monomeric 43 kDa form.

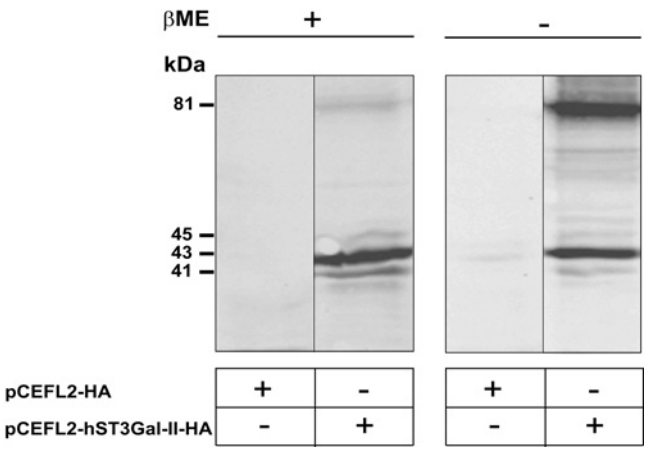

Figure 3 Expression of HA epitope-tagged ST3Gal-II

CHO-K1 cell homogenates (40 μg) transiently transfected with expression vector alone (pCEFL2-HA) or with vector encoding human ST3Gal-II (pCEFL2-hST3Gal-II-HA) were separated by SDS/PAGE (12 % gels) with (+) or without (−) 5 % 2-mercaptoethanol (βME) in the sample buffer and processed as described in the 'Western blotting' Experimental section. Molecular masses in kDa are shown on the left.

To investigate the subcellular localization of ST3Gal-II, particularly at the sub-Golgi complex level, immunostaining of the myc epitope-tagged ST3Gal-II with markers of proximal Golgi complex (ST8Sia-I, GM130), TGN (TGN38) and TGN and late endosomes [M6PR (mannose 6-phosphate receptor)] was carried out. As shown in Figure 4, ST3Gal-II was found predominantly located in a perinuclear region, co-localizing partially with ST8Sia-I (80 %) and GM130 (80 %). Thus these results revealed a broad distribution of ST3Gal-II along the Golgi complex, including the TGN, as was evident from partial co-localization with the specific marker TGN38 (30 %) and M6PR (40 %).

To study further the co-localization of ST3Gal-II and the Golgi markers, cells were treated with BFA (brefeldin A), a fungal macrocyclic lactone that reversibly blocks intra-Golgi vesicular transport, causing redistribution of proximal Golgi membranes (*cis*, *medial* and *trans*), but not TGN membranes, into the endoplasmic reticulum [30,31]. BFA led to a dispersion of most ST3Gal-II throughout the endoplasmic reticulum, increasing its co-localization with endoplasmic reticulum marker Iip33 (Figure 5). As expected, ST3Gal-II and ST8Sia-I, which co-localized at the proximal Golgi complex, redistributed into the endoplasmic reticulum after BFA treatment. It may be argued that the presence of ST3Gal-II in the proximal Golgi is due to mislocalization of overexpressed protein in the transiently transfected cells, as was shown to occur with β4GalNAcT-I [32]. However, the same sub-Golgi localization and behaviour to BFA treatment was observed in CHO-K1 cells stably expressing myc-tagged ST3Gal-II (Figure 5). Thus these experiments reinforce the notion that ST3Gal-II distributes along the Golgi complex, mainly in proximal compartments.

ST3Gal-II depends on N-glycosylation for trafficking to the Golgi complex and enzyme activity

Prediction of N-glycosylation sites in ST3Gal-II was made using the prediction server NetNGlyc 1.0 (http://www.cbs.dtu.dk/services/NetNGlyc/). The enzyme contains two Asn-Xaa-Ser/Thr sequons (Asn^{92} and Asn^{211}) (Figure 2), and the asparagine residue predicted by the algorithm to be N-glycosylated is Asn^{211},

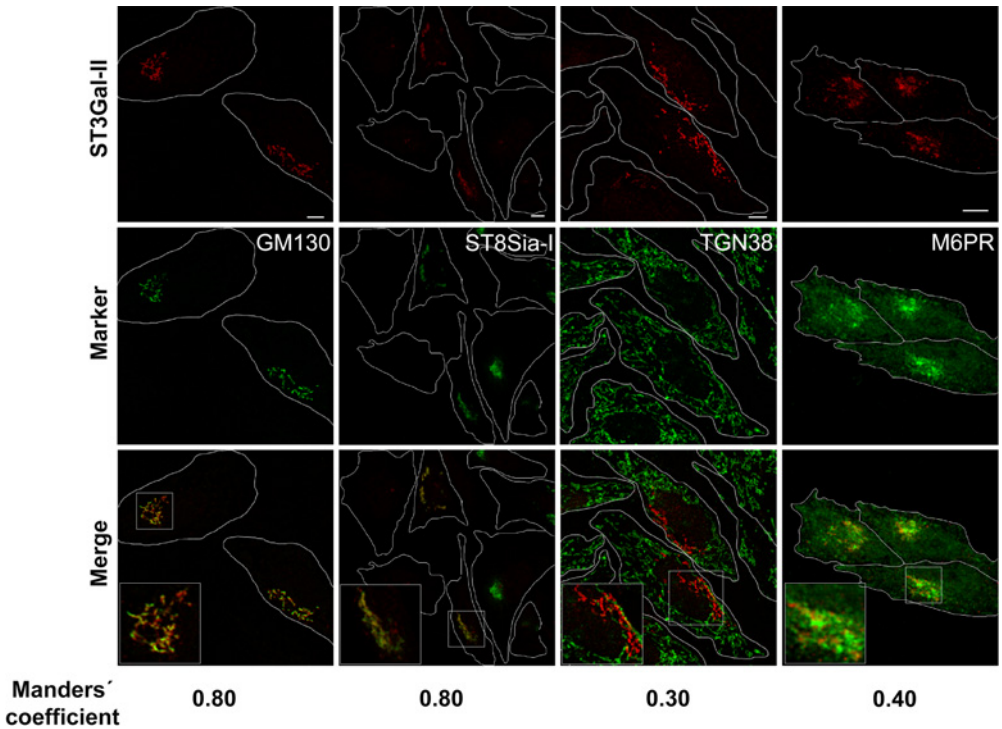

Figure 4 Co-localization of myc epitope-tagged human ST3Gal-II with sub-Golgi complex markers

CHO-K1 cells stably expressing ST3Gal-II–myc were incubated with specific antibodies against GM130 (*cis*-Golgi marker), TGN38 (TGN marker) or M6PR (TGN/late endosome marker). In another set of experiments, these cells were transfected to transiently express ST8Sia-I–YFP (*cis*/*medial*-Golgi marker). Polyclonal rabbit antibody against c-myc was used for detection of ST3Gal-II–myc. Primary antibodies were detected using specific Alexa Fluor-conjugated antibodies as indicated in the Experimental section. Expression of ST8Sia-I was detected by the intrinsic fluorescence of YFP. Cell boundaries (white lines) are indicated. Merged images are shown in the bottom row. Insets in merged panels show details at higher magnification. Manders's co-localization coefficients were calculated using ImageJ software. Scale bars, 5 μm.

whereas the prediction for Asn^{92} N-glycosylation was below the threshold. Additionally, it should be mentioned that the presence of the proline residue (Pro^{95}) at the $+3$ position with respect to Asn^{92} is indicative of a strong, but not absolute, inhibition of N-glycosylation [33].

Initially, we observed that the *en bloc* N-glycosylation inhibitor tunicamycin drastically affected the exiting of ST3Gal-II from the endoplasmic reticulum, strongly suggesting that the enzyme is N-glycosylated and that this co-translational modification is necessary for proper folding and trafficking to the Golgi complex (Figure 6A). In addition, the molecular mass of the polypeptide synthesized in the presence of tunicamycin (41 kDa) was as expected as calculated from the cDNA of ST3Gal-II (Figure 6C), suggesting that at least one potential N-glycosylation site of ST3Gal-II would be occupied by an oligosaccharide (2–3 kDa per each *N*-glycan). Next, to explore whether disturbing the *N*-glycan trimming at the endoplasmic reticulum affects the intracellular trafficking of ST3Gal-II, cells expressing the enzyme were treated with castanospermine, an inhibitor of glucosidase I and II. As shown in Figures 6(A) and 6(B), this inhibitor also impaired the arriving of the sialyltransferase to the Golgi complex with retention at the endoplasmic reticulum, but did not significantly modify its molecular mass (Figure 6C). In control experiments, we observed that cell treatment with tunicamycin or castonospermine did not significantly modify the Golgi complex morphology and distribution of the GM130 protein marker (Figure 6A). Thus these pharmacological studies strongly suggest that ST3Gal-II is being N-glycosylated and that glycosylation is necessary for proper intracellular sorting of the enzyme.

To conclusively confirm that ST3Gal-II is N-glycosylated and determine the impact of this modification on the intracellular transport of this protein, we modified the N-glycosylation sequons of ST3Gal-II by replacing asparagine residues (Asn^{92} and Asn^{211}) in the consensus sequences for N-glycosylation with glutamine residues using site-directed mutagenesis of a plasmid encoding the full-length ST3Gal-II C-terminally tagged with the HA epitope. As shown in Figure 7(A), mutation of the N-glycosylation site at position Asn^{211} (N211Q) resulted in near total retention of ST3Gal-II at the endoplasmic reticulum. A similar result was observed in the protein carrying a double-asparagine mutation (N92Q/N211Q). Surprisingly, mutation of the N-glycosylation site at Asn^{92} (N92Q) did not alter Golgi localization of ST3Gal-II and did not significantly change the molecular mass of the polypeptide when analysed by Western blotting (Figure 7B). In contrast, mutation of Asn^{211} mostly resulted in a polypeptide with a molecular mass expected for a non-glycosylated form (41 kDa) and a minor band (2 %) which probably correspond to ST3Gal-II slightly glycosylated at Asn^{92} (43 kDa). The double-asparagine mutant resulted in a polypeptide with a molecular mass of 41 kDa (Figure 7B). These data indicate that ST3Gal-II is mostly N-glycosylated at Asn^{211} and that this co-translational modification is critical for its proper exit from the endoplasmic reticulum and Golgi localization. N-glycosylation of ST3Gal-II was confirmed further by *in vitro* digestion with PNGase F. PNGase F cleaves N-linked oligosaccharides, regardless of their complexity, by hydrolysing the asparagine oligosaccharide bond. As shown in Figure 7(C), treatment of ST3Gal-II with PNGase F caused a reduction in its molecular mass from 43 kDa to 41 kDa,

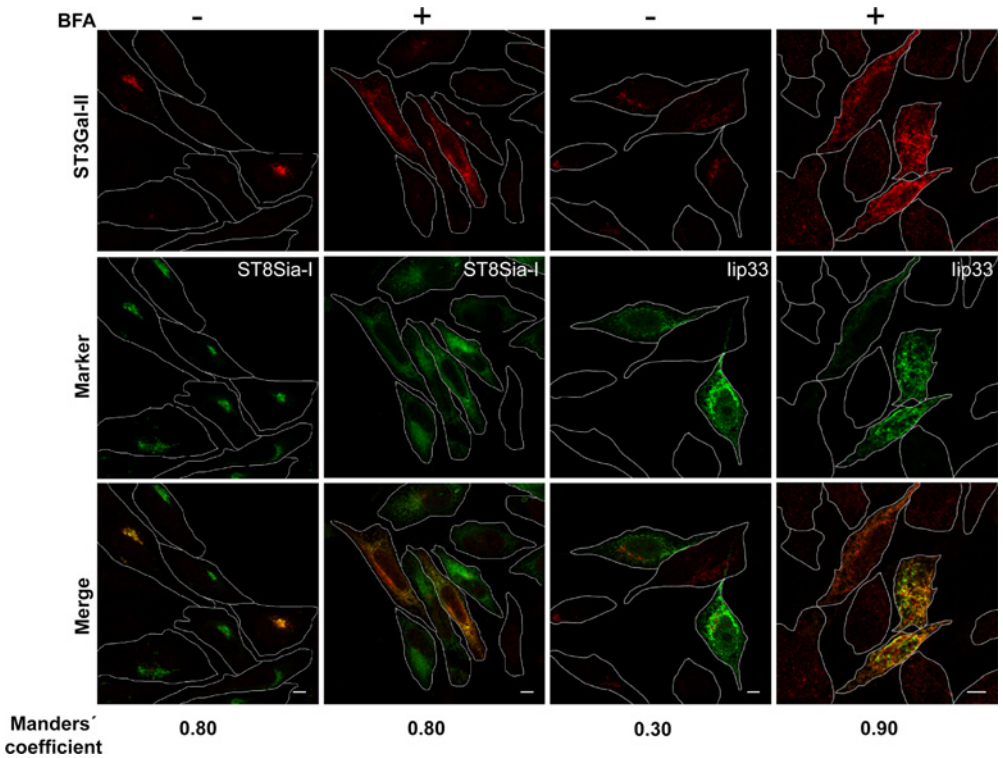

Figure 5 Effect of BFA on ST3Gal-II subcellular localization

CHO-K1 cells stably expressing ST8Sia-I–YFP were transfected to express ST3Gal-II–myc and treated (+) or not (−) with BFA (2 μg/ml) at 37 °C for 30 min. On the other hand, CHO-K1 cells stably expressing ST3Gal-II–myc were transfected with lip33–YFP (endoplasmic-reticulum-resident type II transmembrane protein) and then treated (+) or not (−) with BFA as indicated above. Rabbit anti-c-myc polyclonal antibody was used for detection of ST3Gal-II–myc. Expression of ST8Sia-I and lip33 was detected by the intrinsic fluorescence of YFP. Cell boundaries (white lines) are indicated. Merged images are shown in the bottom row. Manders's co-localization coefficients were calculated using ImageJ software. Scale bars, 5 μm.

similarly to ST3Gal-II carrying a double-asparagine mutation (N92Q/N211Q).

The enzymatic activities were also compared between the wild-type ST3Gal-II and the N-glycosylation mutants. Using glycolipid as acceptor substrate, ST3Gal-II (N211Q) retained 47 % of the activity of the wild-type protein (Figure 8A) while the double mutant (N92Q/N211Q) exhibited only 24 % of the enzyme activity. On the other hand, the single *N*-glycan mutant at Asn^{92} increased to some extent the activity of the enzyme. Interestingly, we observed that the N-glycosylation status of ST3Gal-II also affected enzyme activity towards glycoprotein (Figure 8B). Using asialofetuin as acceptor substrate, ST3Gal-II (N211Q) retained 29 % of the activity of the wild-type protein, whereas the double mutant (N92Q/N211Q) exhibited only 24 % of the enzyme activity. Thus the *N*-glycan at Asn^{211} seems to influence substrate recognition or, eventually, conformational events which are necessary for proper enzyme activity.

N-glycan-processing status

As a complementary approach to investigate the sub-Golgi location of ST3Gal-II, we examined the processing status of its *N*-glycan at Asn^{211}. It is known that glycoproteins moving along the secretory pathway and progressing beyond the *medial*-Golgi suffer the successive action of the processing enzymes N-acetylglucosaminyltransferase I/mannosidase II, acquiring Endo H resistance and terminal glycosylation of their *N*-glycans. Treatment of ST3Gal-II with Endo H caused a reduction of its molecular mass from 43 to 41 kDa (Figure 9), again indicating N-glycosylation at Asn^{211} and that this oligosaccharide contains a high proportion of mannose residues. Interestingly, the molecular mass of Endo H-treated ST3Gal-II was similar to both the polypeptide synthesized in the presence of tunicamycin and ST3Gal-II carrying a double-asparagine mutation (N92Q/N211Q). The result also indicates that most ST3Gal-II does not progress beyond the *medial*-Golgi and supports the sub-Golgi localization of the sialyltransferase demonstrated by confocal microscopy and pharmacological analysis.

The N-terminal, non-glycosylated, region of ST3Gal-II directs the Golgi complex localization of a chimaeric protein

Many studies have indicated that determinants residing in the N-terminal domain of type II transmembrane proteins are involved in their localization at the Golgi complex. Specifically, it was demonstrated for ganglioside glycosyltransferases that the main mechanism of Golgi retention involved their transmembrane domain; and that N-glycosylation is not an absolute requirement for Golgi localization [1,4,34]. To examine these aspects in human ST3Gal-II further, a chimaera was constructed in which the N-terminus of the protein containing the cytosolic, transmembrane and the stem region (amino acids 1–51) was fused to the cherry fluorescent protein, replacing the *N*-glycan bearing C-terminal domain of ST3Gal-II ($ST3Gal\text{-}II^{1-51}$–cherry). The results shown in Figure 10(A) indicate that the N-terminal ST3Gal-II domain was able to drive the fluorescent protein out of the endoplasmic reticulum and to retain it in the Golgi complex. Additionally,

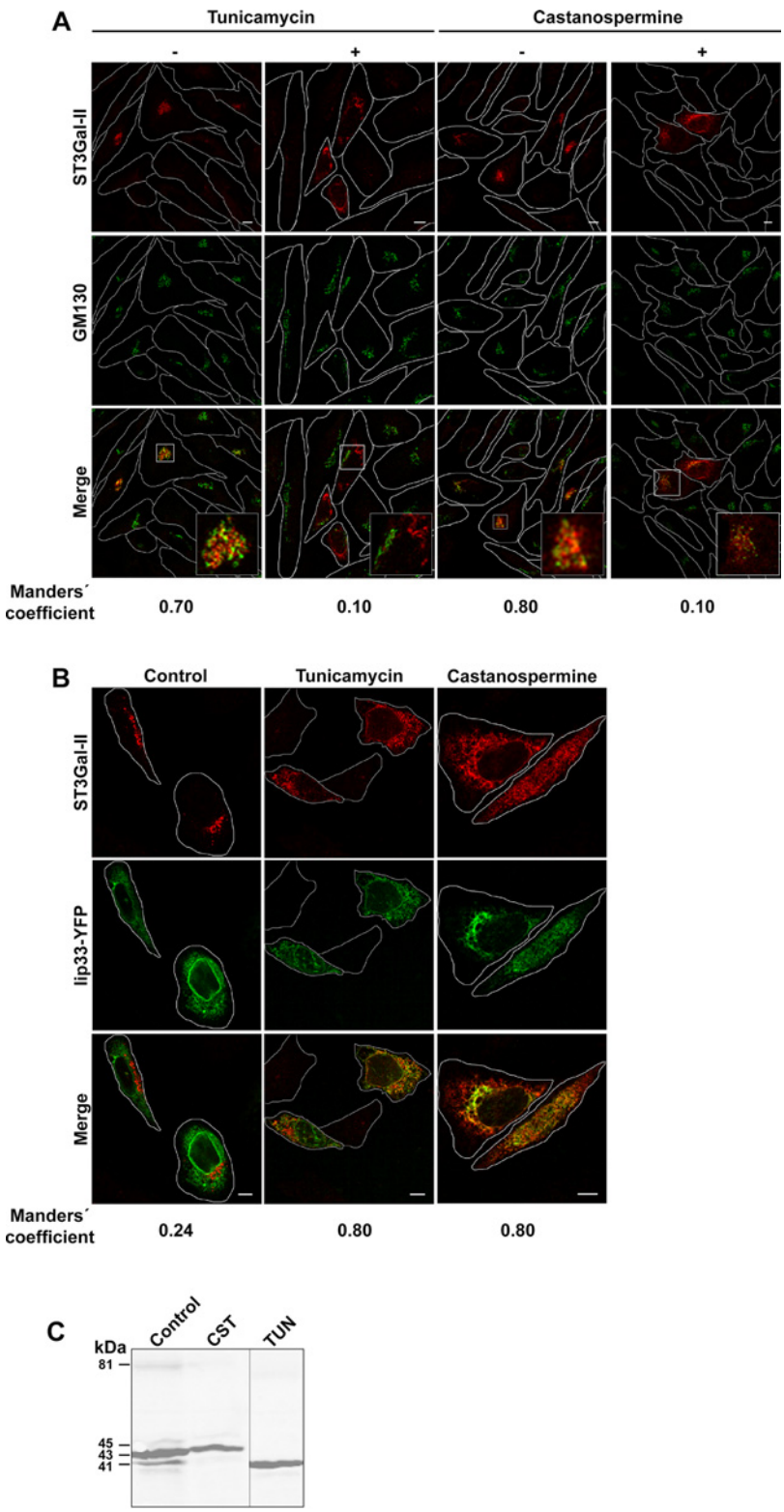

Figure 6 Effect of tunicamycin and castanospermine on ST3Gal-II subcellular localization and N-glycosylation

(**A**) CHO-K1 cells transiently transfected to express ST3Gal-II–HA were treated (+) or not (−) with 10 μg/ml tunicamycin or 75 μg/ml castanospermine, and immunostained to detect ST3Gal-II–HA and GM130 (Golgi marker) as indicated in the Experimental section. Cell boundaries (white lines) are indicated. Merged images are shown in the bottom row. Insets in merged panels show details at higher magnification. Manders's co-localization coefficients are shown at the bottom. Scale bars, 5 μm. (**B**) CHO-K1 cells were co-transfected to express ST3Gal-II–HA and lip33–YFP (endoplasmic-reticulum-resident type II transmembrane protein) and then treated with castanospermine or tunicamycin as indicated above. Merged images are shown in the bottom row. Manders's co-localization coefficients are shown at the bottom. lip33 was detected by the intrinsic fluorescence of YFP. Scale bars, 5 μm. (**C**) Homogenates from cells expressing ST3Gal-II–HA in the presence or absence of added castanospermine (CST) or tunicamycin (TUN) were resolved by SDS/PAGE and probed with anti-HA monoclonal antibody. Molecular masses in kDa are shown on the left.

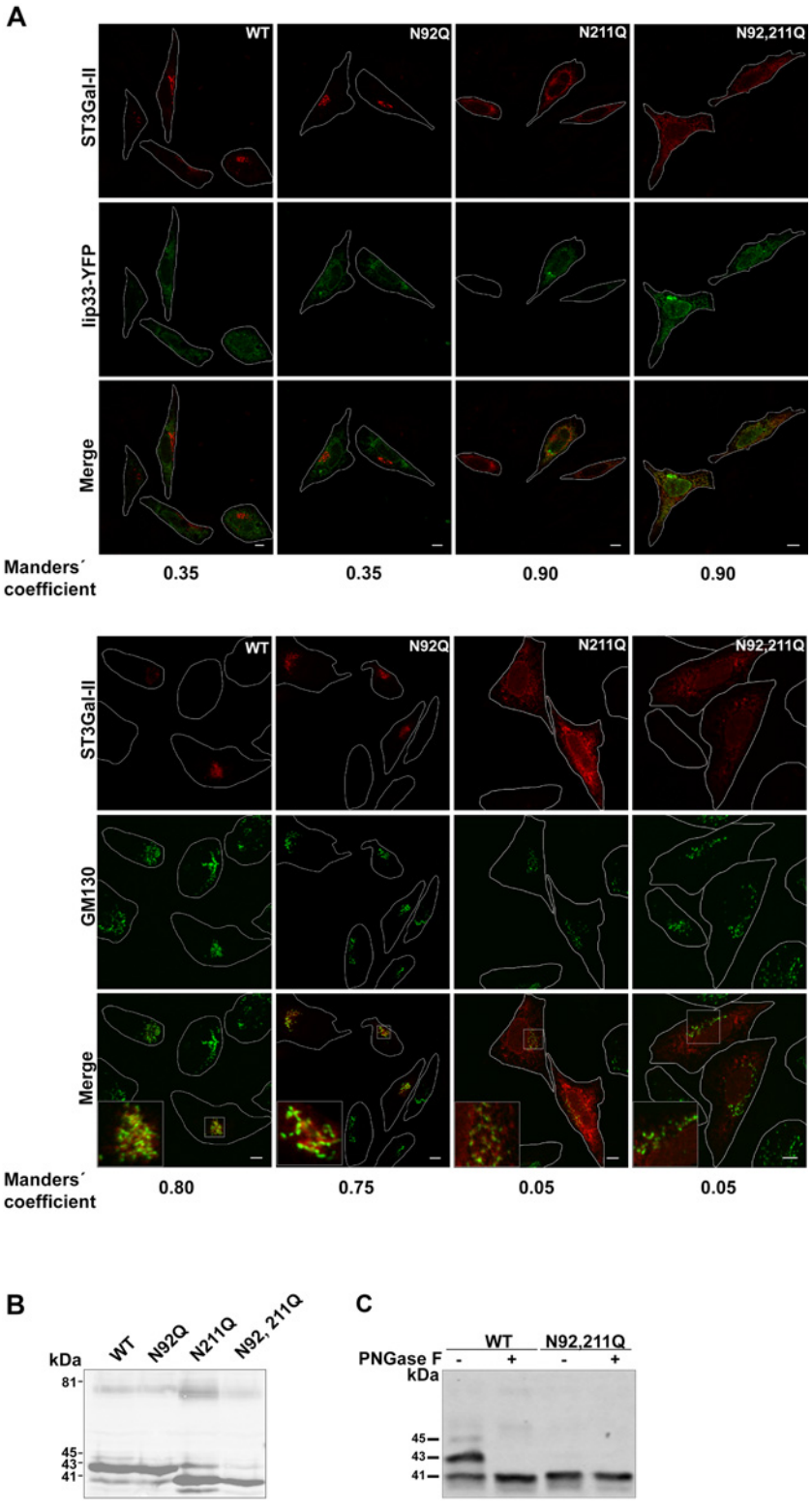

Figure 7 Expression and subcellular localization analysis of wild-type and N-glycosylation mutants of ST3Gal-II

(**A**) CHO-K1 cells were transfected to express wild-type ST3Gal-II–HA or its N-glycosylation mutant variants N92Q, N211Q and N92Q/N211Q, then were fixed, permeabilized and immunostained to detect ST3Gal–HA and GM130 (Golgi complex marker) before examination by confocal fluorescence microscopy. Additionally, these cells were transfected with Iip33–YFP (endoplasmic reticulum marker) and then treated as indicated above. Cell boundaries (white lines) are indicated. Scale bars, 5 μm. (**B**) Total proteins from wild-type or N-glycosylation mutant variants transfected cells were resolved by SDS/PAGE (12 % gels) in the presence of 2-mercaptoethanol. Molecular masses in kDa are shown on the left. (**C**) Homogenates from ST3Gal-II-expressing cells were treated or not with PNGase F for 4 h at 37 °C and subjected to Western blotting following the procedures described in the Experimental section. As a control, extracts from cells expressing ST3Gal-II carrying a double-asparagine mutation (N92Q/N211Q) were processed and run simultaneously. Molecular masses in kDa are shown on the left.

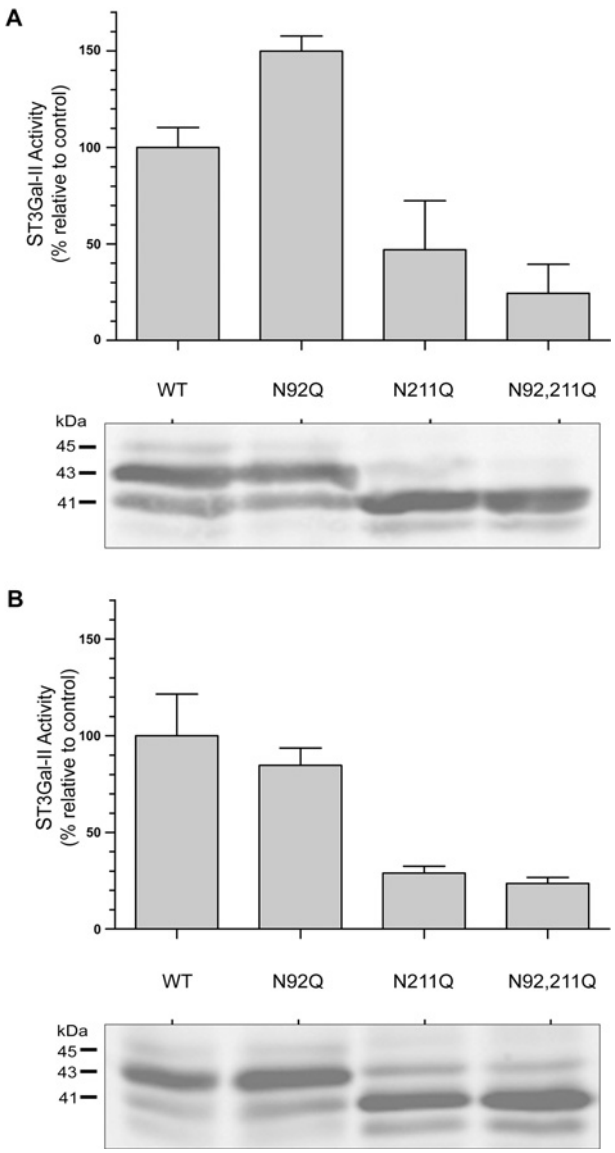

Figure 8 Effect of N-glycosylation on ST3Gal-II enzyme activity

(**A**) Homogenates from CHO-K1 cells expressing wild-type ST3Gal-II and N-glycosylation mutant variants were processed for determination of ST3Gal-II enzyme activity following the procedure described in the Experimental section and using GM1 ganglioside and CMP-9-fluoresceinyl-NeuAc as acceptor and donor substrate respectively. The fluorescent product was extracted and chromatographed on HPTLC plates. The fluorescence intensity obtained in each condition was normalized to ST3Gal-II expression levels which were analysed by Western blotting. A representative blot is shown beneath the histogram with molecular masses indicated in kDa. The enzyme activity was expressed as a percentage relative to the wild-type (WT) ST3Gal-II condition. (**B**) Determination of enzymatic activity of wild-type ST3Gal-II and N-glycosylation mutant variants on glycoproteins was performed using asialofetuin and CMP-9-fluoresceinyl-NeuAc as acceptor and donor substrate respectively. Total proteins were precipitated and the fluorescence intensity obtained in each condition was normalized to ST3Gal-II expression levels which were analysed by Western blotting. A representative blot is shown beneath the histogram with molecular masses indicated in kDa. The enzyme activity was expressed as a percentage relative to the wild-type (WT) ST3Gal-II condition. Results are means±S.E.M. from three independent experiments.

these results also suggest that the C-terminal domain of ST3Gal-II depends on N-glycosylation to attain an optimum conformation for proper exiting from the endoplasmic reticulum and trafficking to the Golgi complex. To scrutinize and confirm these hypotheses further, we performed an additional experiment in which

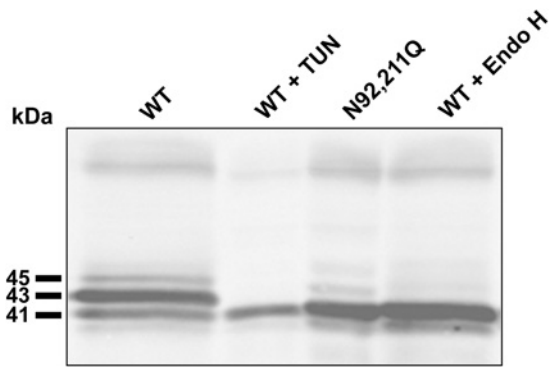

Figure 9 Deglycosylation of ST3Gal-II by Endo H

Homogenates from ST3Gal-II-expressing CHO-K1 cells were treated with Endo H for 18 h at 37 °C and subjected to Western blotting following the procedures described in the Experimental section. As control, extracts from cells expressing wild-type (WT) ST3Gal-II or ST3Gal-II carrying a double-asparagine mutation (N92Q/N211Q) or wild-type ST3Gal-II synthesized in the presence of tunicamycin (TUN) were run and processed simultaneously. Molecular masses in kDa are shown on the left.

CHO-K1 cells were co-transfected to express both the full-length and the short version (ST3Gal-II$^{1-51}$–cherry) of ST3Gal-II. As observed in Figure 10(B), both proteins mostly co-localized at the Golgi complex. However, tunicamycin treatment impaired the arrival of the full-length ST3Gal-II to the Golgi complex with retention in the endoplasmic reticulum, whereas the non-N-glycosylated ST3Gal-II$^{1-51}$–cherry protein version was mostly not affected by the inhibitor. Surprisingly, we observed that in a percentage of double-transfected cells, a fraction of ST3Gal-II$^{1-51}$–cherry protein was retained at the endoplasmic reticulum. This result probably indicates the formation of ST3Gal-II homo-complexes at the endoplasmic reticulum, in which the full-length version of the enzyme might retain the shorter version, as described previously for other ganglioside glycosyltransferases [35].

DISCUSSION

Ganglioside glycosyltransferases have been found to present N-linked oligosaccharides that are essential for their proper subcellular localization and function. For instance, in β3GalT-IV [36], β4GalNAcT-I [37] and ST8Sia-I [38,39], N-glycosylation was found to be necessary for their activity and subcellular localization, probably reflecting known oligosaccharide-mediated quality controls of protein conformation in the endoplasmic reticulum [4,40]. Additionally, N-glycosylation was also demonstrated to occur in glycoprotein glycosyltransferases. In particular, the critical role of N-linked oligosaccharides on the enzymatic properties of human O-glycan core 2 β-1,6-N-acetylglucosaminyltransferase [41] and human α1,3/4-fucosyltransferase III, -V and -VI [42] and on intracellular trafficking and subcellular distribution as for ST6Gal I [11] and N-acetylglucosaminyltransferase III [43] is known. In the present study, by confocal microscopy analysis, pharmacological and biochemical experiments and site-directed mutagenesis, we demonstrated that ST3Gal-II is broadly distributed along the Golgi complex cisternae, mainly in proximal compartments, and is N-glycosylated at Asn^{211}. Our results show that the N-glycosylation-defective mutant of ST3Gal-II decreases both its exit from the endoplasmic reticulum and proper sorting to the Golgi complex, which is probably due to conformational

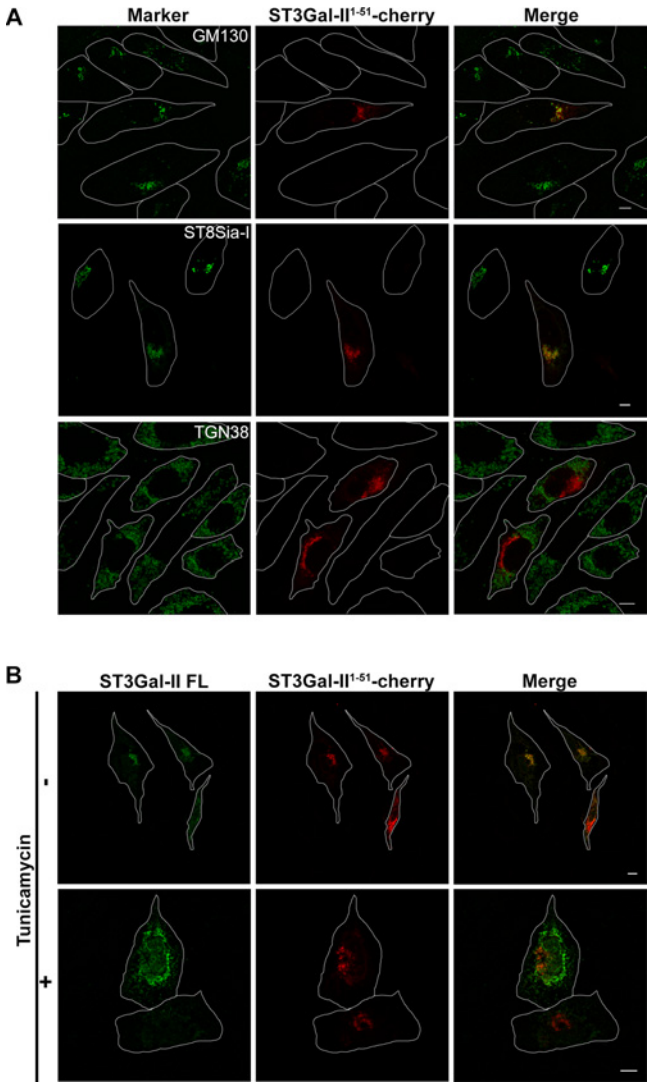

Figure 10 The N-terminal domain (amino acids 1–51) of ST3Gal-II directs the Golgi complex localization of a fluorescent protein

(**A**) A chimaeric protein containing the N-terminal domain of ST3Gal-II fused to the cherry fluorescent protein (ST3Gal-II$^{1-51}$–cherry) was constructed. CHO-K1 cells transiently expressing ST3Gal-II$^{1-51}$–cherry were incubated with specific antibodies against GM130 or TGN38 (*cis*-Golgi and TGN markers respectively). In another set of experiments, CHO-K1 cells were co-transfected to express ST3Gal-II$^{1-51}$–cherry and ST8Sia-I–YFP, a proximal Golgi marker. Primary antibodies were detected using specific Alexa Fluor-conjugated antibodies as described in the Experimental section. Expression of ST8Sia-I–YFP and ST3Gal-II$^{1-51}$–cherry was detected by the intrinsic fluorescence of YFP and cherry fluorescent protein respectively. Scale bars, 5 μm. (**B**) CHO-K1 cells were co-transfected to express full-length ST3Gal-II (ST3Gal-II FL) and ST3Gal-II$^{1-51}$–cherry, treated (+) or not (−) with 10 μg/ml tunicamycin, immunostained and processed for confocal microscopy. Merged images are shown in the rightmost column. Cell boundaries (white lines) are indicated. Scale bars, 5 μm.

changes of ST3Gal-II. Additionally, we also demonstrate that ST3Gal-II required a proper trimming of its *N*-glycan for proper Golgi sorting since inhibition of the endoplasmic-reticulum-resident glucosidase I and II severely affected its exit from this organelle. Endo H treatment showed that most of the ST3Gal-II *N*-glycan was sensitive to the endoglycosidase, which indicates that the oligosaccharide was not of the complex type and contains a high proportion of mannose residues. Additionally, the result also indicates that most ST3Gal-II does not progress beyond the *medial*-Golgi and supports the sub-Golgi localization of the sialyltransferase demonstrated by confocal microscopy and pharmacological analysis.

All eukaryotic sialyltransferases contain certain conserved sequence motifs referred to as sialylmotifs L (large), S (small) and VS (very small) [44,45] (Figure 2A). Later on, an additional motif, denoted as motif III, was found to be located between sialylmotifs S and VS and conserved in all sialyltransferases [12]. More recently, sequence motifs that are unique to the various families of sialyltransferases have been identified [46]. In particularly, ST3Gal family contains two small linkage-specific motifs located between the L- and S-motifs (Figure 2A). These motifs are expected to be important for linkage specificity and for recognizing the monosaccharide moiety that accepts sialic acid [46]. In this sense, it should be remarked that the N-glycosylated Asn^{211} in ST3Gal-II is located between the two family motifs identified, which strongly suggests that this co-translational modification could eventually influence enzymatic properties of the sialyltransferase, as observed in the present study using both glycolipid and glycoprotein as acceptor substrates (Figure 8).

It was demonstrated previously for other ganglioside glycosyltransferases that the main mechanism of Golgi retention involves their transmembrane domain, and that N-glycosylation is not an absolute requirement for Golgi localization [1,4,34]. According to results shown in Figure 10, ST3Gal-II does not seem to be the exception. We observed that the N-terminal ST3Gal-II domain was able to drive a fluorescent protein reporter out of the endoplasmic reticulum and to retain it in the Golgi complex, highlighting the notion that molecular determinants residing at the N-terminal domain drive Golgi localization.

ST3Gal-II was expressed mainly as a disulfide-bonded 81 kDa product, whose formation persisted when exit of the protein from the endoplasmic reticulum was impaired by inhibiting glucosidases I and II with castanospermine, indicating that formation of homodimer occurs mainly in the endoplasmic reticulum (Supplementary Figure S1A). In this regard, disulfide-bonded homodimers of β4GalNAcT-I formed in the endoplasmic reticulum [47] have been described. Interestingly, experiments using the N92Q/N211Q mutant of ST3Gal-II or expression of ST3Gal-II in the presence of tunicamycin indicated that the non-N-glycosylated monomeric version ST3Gal-II is also able to form dimers (Supplementary Figure S1B). Additionally, experiments shown in Figure 10 strongly suggest the formation of ST3Gal-II homo-association at the endoplasmic reticulum since a full-length version of the enzyme, which is retained in this organelle by affecting its N-glycosylation status, was able to retain a truncated (amino acids 1–51) and non-glycosylated version of the enzyme lacking the catalytic domain. In this regard, it was demonstrated by FRET microscopy experiments in living cells that the N-terminal domains of β4GalNAcT-I, a glycosyltransferase involved in the synthesis of GM2, GD2 and GT2 gangliosides, are able to form homocomplexes [35]. Moreover, glycoprotein glycosyltransferases were also found to form homomers and heteromers during their trafficking within the early secretory compartments [48,49]. Although this topic should be investigated further, it was suggested that glycosyltransferase complex formation might be considered as a potential enzymatic activity-regulation mechanism, by fine-tuning the compositions and the stoichiometric relationship between enzymes involved in a particular glycosylation process [4].

In conclusion, we demonstrated that ST3Gal-II is N-glycosylated at predicted N-glycosylation consensus sequences and revealed the role of this glycosylation for its trafficking to the proximal Golgi complex and enzymatic activity. It is worth noting that the GD1a ganglioside, the product of this sialyltransferase, is

a glycolipid target of autoantibodies associated with a wide range of clinically identifiable acute and chronic neuropathy syndromes, including Guillain–Barré and Miller–Fisher syndromes [50–52]. Thus inhibition of ST3Gal-II N-glycosylation might be considered as a new and potential target for neuropathology therapeutics.

AUTHOR CONTRIBUTION

Fernando Ruggiero, Aldo Vilcaes and Ramiro Iglesias-Bartolomé performed experiments. Fernando Ruggiero, Aldo Vilcaes and José Daniotti conceived ideas, designed experiments, analysed results and wrote the paper. All authors edited and reviewed the final paper before submission.

ACKNOWLEDGEMENTS

We thank C. Sampedro, C. Mas, G. Schachner and S. Deza for technical assistance. The antibody against the HA epitope was kindly supplied by Carlos Arregui (IIB-INTECH, Buenos Aires, Argentina). Castanospermine and Endo H was generously supplied by Cecilia D'Alessio (Fundación Instituto Leloir, Buenos Aires, Argentina). We appreciate the generosity of Dr Silvio Gutkind, who allowed us to perform some of the experiments in his laboratory and are grateful for his constant encouragement.

FUNDING

This work was supported in part by the Secretaría de Ciencia y Tecnología (SECyT, 203/14), Universidad Nacional de Córdoba (UNC), Consejo Nacional de Investigaciones Científicas y Técnicas (CONICET, PIP 112-20110100930) and Agencia Nacional de Promoción Científica y Tecnológica (ANPCyT, PICT 2010 N° 1487, PICT 2013 N° 456), Argentina. F.M.R. is a recipient of an ANPCyT and CONICET fellowship. A.A.V. and J.L.D. are career investigators of CONICET (Argentina).

REFERENCES

1 Daniotti, J.L. and Iglesias-Bartolome, R. (2011) Metabolic pathways and intracellular trafficking of gangliosides. IUBMB Life **63**, 513–520 CrossRef PubMed
2 Daniotti, J.L., Vilcaes, A.A., Torres Demichelis, V., Ruggiero, F.M. and Rodriguez-Walker, M. (2013) Glycosylation of glycolipids in cancer: basis for development of novel therapeutic approaches. Front. Oncol. **3**, 306 CrossRef PubMed
3 Yu, R.K., Tsai, Y.T., Ariga, T. and Yanagisawa, M. (2011) Structures, biosynthesis, and functions of gangliosides: an overview. J. Oleo Sci. **60**, 537–544 CrossRef PubMed
4 Maccioni, H.J., Quiroga, R. and Ferrari, M.L. (2011) Cellular and molecular biology of glycosphingolipid glycosylation. J. Neurochem. **117**, 589–602 PubMed
5 Crespo, P.M., Demichelis, V.T. and Daniotti, J.L. (2010) Neobiosynthesis of glycosphingolipids by plasma membrane-associated glycosyltransferases. J. Biol. Chem. **285**, 29179–29190 CrossRef PubMed
6 Sonnino, S., Aureli, M., Loberto, N., Chigorno, V. and Prinetti, A. (2010) Fine tuning of cell functions through remodeling of glycosphingolipids by plasma membrane-associated glycohydrolases. FEBS Lett. **584**, 1914–1922 CrossRef PubMed
7 Vilcaes, A.A., Demichelis, V.T. and Daniotti, J.L. (2011) Trans-activity of plasma membrane-associated ganglioside sialyltransferase in mammalian cells. J. Biol. Chem. **286**, 31437–31446 CrossRef PubMed
8 Apweiler, R., Hermjakob, H. and Sharon, N. (1999) On the frequency of protein glycosylation, as deduced from analysis of the SWISS-PROT database. Biochim. Biophys. Acta **1473**, 4–8 CrossRef PubMed
9 Dennis, J.W., Granovsky, M. and Warren, C.E. (1999) Glycoprotein glycosylation and cancer progression. Biochim. Biophys. Acta **1473**, 21–34 CrossRef PubMed
10 Fares, F. (2006) The role of O-linked and N-linked oligosaccharides on the structure–function of glycoprotein hormones: development of agonists and antagonists. Biochim. Biophys. Acta **1760**, 560–567 CrossRef PubMed
11 Chen, C. and Colley, K.J. (2000) Minimal structural and glycosylation requirements for ST6Gal I activity and trafficking. Glycobiology **10**, 531–583 CrossRef PubMed
12 Jeanneau, C., Chazalet, V., Auge, C., Soumpasis, D.M., Harduin-Lepers, A., Delannoy, P., Imberty, A. and Breton, C. (2004) Structure–function analysis of the human sialyltransferase ST3Gal I: role of N-glycosylation and a novel conserved sialylmotif. J. Biol. Chem. **279**, 13461–13468 CrossRef PubMed
13 Uemura, S., Kurose, T., Suzuki, T., Yoshida, S., Ito, M., Saito, M., Horiuchi, M., Inagaki, F., Igarashi, Y. and Inokuchi, J. (2006) Substitution of the *N*-glycan function in glycosyltransferases by specific amino acids: ST3Gal-V as a model enzyme. Glycobiology **16**, 258–270 CrossRef PubMed
14 Audry, M., Jeanneau, C., Imberty, A., Harduin-Lepers, A., Delannoy, P. and Breton, C. (2011) Current trends in the structure–activity relationships of sialyltransferases. Glycobiology **21**, 716–726 CrossRef PubMed
15 Iwamori, M. and Iwamori, Y. (2005) Changes in the glycolipid composition and characteristic activation of GM3 synthase in the thymus of mouse after administration of dexamethasone. Glycoconj. J. **22**, 119–126 CrossRef PubMed
16 Prinetti, A., Chigorno, V., Mauri, L., Loberto, N. and Sonnino, S. (2007) Modulation of cell functions by glycosphingolipid metabolic remodeling in the plasma membrane. J. Neurochem. **103**, 113–125 CrossRef PubMed
17 Kono, M., Ohyama, Y., Lee, Y.C., Hamamoto, T., Kojima, N. and Tsuji, S. (1997) Mouse β-galactoside α2,3-sialyltransferases: comparison of *in vitro* substrate specificities and tissue specific expression. Glycobiology **7**, 469–479 CrossRef PubMed
18 Lee, Y.C., Kurosawa, N., Hamamoto, T., Nakaoka, T. and Tsuji, S. (1993) Molecular cloning and expression of Gal β1,3GalNAc α2,3-sialyltransferase from mouse brain. Eur. J. Biochem. **216**, 377–385 CrossRef PubMed
19 Giordanengo, V., Bannwarth, S., Laffont, C., Van Miegem, V., Harduin-Lepers, A., Delannoy, P. and Lefebvre, J.C. (1997) Cloning and expression of cDNA for a human Gal(β1–3)GalNAc α2,3-sialyltransferase from the CEM T-cell line. Eur. J. Biochem. **247**, 558–566 CrossRef PubMed
20 Petit, D., Teppa, E., Mir, A.M., Vicogne, D., Thisse, C., Thisse, B., Filloux, C. and Harduin-Lepers, A. (2015) Integrative view of α2,3-sialyltransferases (ST3Gal) molecular and functional evolution in deuterostomes: significance of lineage-specific losses. Mol. Biol. Evol. **32**, 906–927 CrossRef PubMed
21 Lehmann, F., Kelm, S., Dietz, F., von Itzstein, M. and Tiralongo, J. (2008) The evolution of galactose α2,3-sialyltransferase: *Ciona intestinalis* ST3GAL I/II and *Takifugu rubripes* ST3GAL II sialylate Galβ1,3GalNAc structures on glycoproteins but not glycolipids. Glycoconj. J. **25**, 323–334 CrossRef PubMed
22 Kojima, N., Lee, Y.C., Hamamoto, T., Kurosawa, N. and Tsuji, S. (1994) Kinetic properties and acceptor substrate preferences of two kinds of Gal β1,3GalNAc α2,3-sialyltransferase from mouse brain. Biochemistry **33**, 5772–5776 CrossRef PubMed
23 Sturgill, E.R., Aoki, K., Lopez, P.H., Colacurcio, D., Vajn, K., Lorenzini, I., Majic, S., Yang, W.H., Heffer, M., Tiemeyer, M. et al. (2012) Biosynthesis of the major brain gangliosides GD1a and GT1b. Glycobiology **22**, 1289–1301 CrossRef PubMed
24 Toivonen, S., Aitio, O. and Renkonen, O. (2001) α2,3-Sialylation of terminal GalNAc β1–3Gal determinants by ST3Gal II reveals the multifunctionality of the enzyme: the resulting Neu5Ac α2–3GalNAc linkage is resistant to sialidases from Newcastle disease virus and *Streptococcus pneumoniae*. J. Biol. Chem. **276**, 37141–37148 CrossRef PubMed
25 Chandrasekaran, E.V., Xue, J., Xia, J., Locke, R.D., Matta, K.L. and Neelamegham, S. (2008) Reversible sialylation: synthesis of cytidine 5′-monophospho-*N*-acetylneuraminic acid from cytidine 5′-monophosphate with α2,3-sialyl O-glycan-, glycolipid-, and macromolecule-based donors yields diverse sialylated products. Biochemistry **47**, 320–330 CrossRef PubMed
26 Spessott, W., Crespo, P.M., Daniotti, J.L. and Maccioni, H.J. (2012) Glycosyltransferase complexes improve glycolipid synthesis. FEBS Lett. **586**, 2346–2350 CrossRef PubMed
27 Gross, H.J. (1992) Fluorescent CMP-sialic acids as a tool to study the specificity of the CMP-sialic acid carrier and the glycoconjugate sialylation in permeabilized cells. Eur. J. Biochem. **203**, 269–275 CrossRef PubMed
28 Daniotti, J.L., Rosales Fritz, V., Kunda, P., Nishi, T. and Maccioni, H.J. (1997) Cloning, characterization and developmental expression of α2,8 sialyltransferase (GD3 synthase, ST8Sia I) gene in chick brain and retina. Int. J. Dev. Neurosci. **15**, 767–776 CrossRef PubMed
29 Rosales Fritz, V.M., Daniotti, J.L. and Maccioni, H.J. (1997) Chinese hamster ovary cells lacking GM1 and GD1a synthesize gangliosides upon transfection with human GM2 synthase. Biochim. Biophys. Acta **1354**, 153–158 CrossRef PubMed
30 Donaldson, J.G. and Klausner, R.D. (1994) ARF: a key regulatory switch in membrane traffic and organelle structure. Curr. Opin. Cell Biol. **6**, 527–532 CrossRef PubMed
31 Mossessova, E., Corpina, R.A. and Goldberg, J. (2003) Crystal structure of ARF1*Sec7 complexed with Brefeldin A and its implications for the guanine nucleotide exchange mechanism. Mol. Cell **12**, 1403–1411 CrossRef PubMed
32 Giraudo, C.G., Rosales Fritz, V.M. and Maccioni, H.J. (1999) GA2/GM2/GD2 synthase localizes to the trans-Golgi network of CHO-K1 cells. Biochem. J. **342**, 633–640 CrossRef PubMed
33 Ben-Dor, S., Esterman, N., Rubin, E. and Sharon, N. (2004) Biases and complex patterns in the residues flanking protein N-glycosylation sites. Glycobiology **14**, 95–101 CrossRef PubMed
34 Maccioni, H.J., Daniotti, J.L. and Martina, J.A. (1999) Organization of ganglioside synthesis in the Golgi apparatus. Biochim. Biophys. Acta **1437**, 101–118 CrossRef PubMed

35 Ferrari, M.L., Gomez, G.A. and Maccioni, H.J. (2012) Spatial organization and stoichiometry of N-terminal domain-mediated glycosyltransferase complexes in Golgi membranes determined by fret microscopy. Neurochem. Res. **37**, 1325–1334 CrossRef PubMed
36 Martina, J.A., Daniotti, J.L. and Maccioni, H.J. (2000) GM1 synthase depends on N-glycosylation for enzyme activity and trafficking to the Golgi complex. Neurochem. Res. **25**, 725–731 CrossRef PubMed
37 Haraguchi, M., Yamashiro, S., Furukawa, K., Takamiya, K. and Shiku, H. (1995) The effects of the site-directed removal of N-glycosylation sites from β-1,4-N-acetylgalactosaminyltransferase on its function. Biochem. J. **312**, 273–280 PubMed
38 Daniotti, J.L., Martina, J.A., Giraudo, C.G., Zurita, A.R. and Maccioni, H.J. (2000) GM3 α2,8-sialyltransferase (GD3 synthase): protein characterization and sub-Golgi location in CHO-K1 cells. J. Neurochem. **74**, 1711–1720 CrossRef PubMed
39 Martina, J.A., Daniotti, J.L. and Maccioni, H.J. (1998) Influence of N-glycosylation and *N*-glycan trimming on the activity and intracellular traffic of GD3 synthase. J. Biol. Chem. **273**, 3725–3731 CrossRef PubMed
40 D'Alessio, C., Caramelo, J.J. and Parodi, A.J. (2010) UDP-GIC:glycoprotein glucosyltransferase-glucosidase II, the yin–yang of the ER quality control. Semin. Cell Dev. Biol. **21**, 491–499 CrossRef PubMed
41 Toki, D., Sarkar, M., Yip, B., Reck, F., Joziasse, D., Fukuda, M., Schachter, H. and Brockhausen, I. (1997) Expression of stable human O-glycan core 2 β-1,6-N-acetylglucosaminyltransferase in Sf9 insect cells. Biochem. J. **325**, 63–69 PubMed
42 Christensen, L.L., Jensen, U.B., Bross, P. and Orntoft, T.F. (2000) The C-terminal N-glycosylation sites of the human α1,3/4-fucosyltransferase III, -V, and -VI (hFucTIII, -V, and -VI) are necessary for the expression of full enzyme activity. Glycobiology **10**, 931–939 CrossRef PubMed
43 Nagai, K., Ihara, Y., Wada, Y. and Taniguchi, N. (1997) N-glycosylation is requisite for the enzyme activity and Golgi retention of N-acetylglucosaminyltransferase III. Glycobiology **7**, 769–776 CrossRef PubMed
44 Datta, A.K. and Paulson, J.C. (1997) Sialylmotifs of sialyltransferases. Indian J. Biochem. Biophys. **34**, 157–165 PubMed
45 Geremia, R.A., Harduin-Lepers, A. and Delannoy, P. (1997) Identification of two novel conserved amino acid residues in eukaryotic sialyltransferases: implications for their mechanism of action. Glycobiology **7**, v–vii CrossRef
46 Patel, R.Y. and Balaji, P.V. (2006) Identification of linkage-specific sequence motifs in sialyltransferases. Glycobiology **16**, 108–116 CrossRef PubMed
47 Jaskiewicz, E., Zhu, G., Taatjes, D.J., Darling, D.S., Zwanzig, Jr, G.E. and Young, Jr, W.W. (1996) Cloned β1,4N-acetylgalactosaminyltransferase: subcellular localization and formation of disulfide bonded species. Glycoconj. J. **13**, 213–223 CrossRef PubMed
48 Hassinen, A. and Kellokumpu, S. (2014) Organizational interplay of Golgi N-glycosyltransferases involves organelle microenvironment-dependent transitions between enzyme homo- and heteromers. J. Biol. Chem. **289**, 26937–26948 CrossRef PubMed
49 Hassinen, A., Rivinoja, A., Kauppila, A. and Kellokumpu, S. (2010) Golgi N-glycosyltransferases form both homo- and heterodimeric enzyme complexes in live cells. J. Biol. Chem. **285**, 17771–17777 CrossRef PubMed
50 Fewou, S.N., Rupp, A., Nickolay, L.E., Carrick, K., Greenshields, K.N., Pediani, J., Plomp, J.J. and Willison, H.J. (2012) Anti-ganglioside antibody internalization attenuates motor nerve terminal injury in a mouse model of acute motor axonal neuropathy. J. Clin. Invest. **122**, 1037–1051 CrossRef PubMed
51 Lardone, R.D., Yuki, N., Odaka, M., Daniotti, J.L., Irazoqui, F.J. and Nores, G.A. (2010) Anti-GM1 IgG antibodies in Guillain–Barré syndrome: fine specificity is associated with disease severity. J. Neurol. Neurosurg. Psychiatry **81**, 629–633 CrossRef PubMed
52 Willison, H.J. and Yuki, N. (2002) Peripheral neuropathies and anti-glycolipid antibodies. Brain **125**, 2591–2625 CrossRef PubMed
53 Svennerholm, L. (1980) Ganglioside designation. Adv. Exp. Med. Biol. **125**, 11 CrossRef PubMed

Received 17 January 2015/21 April 2015; accepted 28 April 2015
Published as BJ Immediate Publication 28 April 2015, doi:10.1042/BJ20150072